Control of dark current in photoelectrochemical (TiO_2/I^-–I_3^-) and dye-sensitized solar cells

Seigo Ito,* Paul Liska, Pascal Comte, Raphaël Charvet, Peter Péchy, Udo Bach, Lukas Schmidt-Mende, Shaik Mohammed Zakeeruddin, Andreas Kay, Mohammad K. Nazeeruddin and Michael Grätzel

Received (in Cambridge, UK) 25th April 2005, Accepted 1st July 2005
First published as an Advance Article on the web 2nd August 2005
DOI: 10.1039/b505718c

The ruthenium complex bis-tetrabutylammonium *cis*-dithiocyanato-*N*,*N*′-bis-2,2′-bipyridine-4-carboxylic acid, 4′-carboxylate ruthenium(II), N-719, was found to block the dark current of dye sensitized solar cells (DSC), based on mesoporous TiO_2 films deposited on a F-doped tin oxide electrode and the effect was compared to surface treatment by $TiCl_4$ and the introduction of a compact TiO_2 blocking layer.

Controlling the dark current in dye-sensitized solar cells (DSC) is very important due to the scientific and industrial interest to enhance the photoenergy conversion efficiency. In a DSC using I^-/I_3^- as a redox couple, charge recombination between photoinjected electrons in TiO_2 and the oxidized dye is negligible, because the regeneration of the sensitizer by I^- is significantly faster than the charge transfer from TiO_2 to the oxidized dye.[1] Hence, preventing the recapture of photoinjected electrons by I_3^- is critical to obtain a high open circuit photovoltage. In order to prevent the charge recombination, previous investigations concerned core shell structured mesoscopic electrodes,[2] surface silanization,[3] an amphiphilic coadsorbent[4] and a TiO_2 underlayer on fluorine-doped SnO_2 transparent conducting oxide (FTO) glass substrate.[5]

Concerning the effect of the underlayer, while significant progresses have been made in understanding the electron transport and recombination in the mesoporous oxide film, the detailed mechanism is still under debate. Kay[5a] suggested that, although a thin layer of TiO_2 prepared by hydrolysis of titanium butoxide reduces somewhat the dark current, the dark current due to the FTO substrate is negligible compared to that of the dye-coated porous TiO_2 film, because the dark current from the dye-coated porous TiO_2 film was extremely higher than that from FTO. Ito *et al.*[5b] found the increase in open-circuit photovoltage (V_{OC}) by introducing a nanocrystalline TiO_2 underlayer between the FTO and meso-macroporous TiO_2 layers. Cameron and Peter reported at first that introducing a compact TiO_2 layer between the FTO and the nanocrystalline film did not affect the V_{OC}.[5c] However, in their latest reports, the compact TiO_2 layer improved the V_{OC} slightly under one sun.[5d,e] Moreover, from intensity-modulated infrared spectroscopy (IMIS) analysis, Frank *et al.*[6] concluded that recombination occurs predominantly near the FTO substrate and not across the entire TiO_2 film, which suggests the usefulness of the TiO_2 underlayer on FTO.

Laboratoire de Photonique et Interfaces, Institut des Sciences et Ingénierie Chimiques, École Polytechnique Fédérale de Lausanne, Station 6, CH-1015 Lausanne, Switzerland. E-mail: seigo.ito@epfl.ch; Fax: +41-21-693-4111; Tel: +41-21-693-3115

In this study, we report on the influence of different surface treatments on the dark and photocurrent performance in high-efficiency (>10%) DSCs. These surface treatments include the ruthenium dye adsorption and $TiCl_4$ treatment of the FTO conductive glass support and the nanocrystalline TiO_2 layer, respectively, as well as the introduction of an additional compact TiO_2 underlayer (UL) between those two layers.

For the photovoltaic experiments, four types of TiO_2 working electrodes were prepared on FTO (10 Ω/□, Nippon Sheet Glass). The first type of working electrode, denoted <nano-TiO_2>, is a double layer of mesoporous TiO_2 coated by screen-printing on the FTO (diameter of TiO_2 nanoparticles: 20 nm; thickness of nanocrystalline TiO_2 layer: 14 μm, thickness of microncrystalline TiO_2 layer: 4 μm).[4] The second type of electrode designated as <$TiCl_4$/nano-TiO_2/$TiCl_4$> was prepared by treating the electrode with $TiCl_4$. The $TiCl_4$ treatments were performed by soaking each electrode in 40 mM $TiCl_4$ aqueous solution at 70 °C for 30 min. The $TiCl_4$ treatment was performed twice, *i.e.* before and after depositing the mesoporous TiO_2 in order to examine its influence on the FTO. The third type of electrode called <UL/nano-TiO_2> employed a compact-TiO_2-underlayer (UL) deposited by spray pyrolysis[7] between the porous TiO_2 and the FTO. Spray-coated ULs have been successfully used for solid-state DSC, hence the spray-coated UL has significant influence for optimal coating on the FTO surface.[8] The fourth kind of electrode designated as <UL/nano-TiO_2/$TiCl_4$>) was identical to the third type except that an additional treatment with $TiCl_4$ was performed.

The N719: Ru dye[9] was adsorbed by soaking the above electrodes after sintering in a 0.5 mM Ru dye solution in acetonitrile/*tert*-butanol (50/50, v/v) for 24 h. The stained electrodes are designated as "<TiO_2film/Ru-dye>". Pt counter electrodes were prepared by coating a drop of H_2PtCl_6 solution on the FTO and heating at 400 °C for 15 min. Cells were sealed by using hot-melt ionomer films of Surlyn 1702 (DuPont). The electrolyte contained 0.60 M 1-methyl-3-butyl-imidazolium iodide, 0.03 M I_2, 0.10 M guanidinium thiocyanate and 0.50 M 4-*tert*-butylpyridine a mixed solvent of acetonitrile and valeronitrile (volume ratio: 85 : 15). To improve and stabilize the photovoltaic performances, an anti-reflection and UV-cut off film ($\lambda < 380$ nm, ARKTOP, ASAHI GLASS) was attached to the DSC surface.

Table 1 shows the characteristics of porous TiO_2 electrodes with/without $TiCl_4$ treatments. The average pore diameter and specific surface area decreased with the $TiCl_4$ treatment, because of the surface epitaxial growth of TiO_2 from $TiCl_4$ entirely on original TiO_2 nanocrystals, resulting in particle-necking and a new TiO_2

Table 1 Characteristics of nanocrystalline TiO_2 layers with dependence on $TiCl_4$ treatment. Each datum, which was calculated to "par 1 μm", was the average of three samples, except for the BET measurements: specific surface area and average pore size

Electrodes	Nano-TiO_2	$TiCl_4$-treated nano-TiO_2
Average pore diameter/nm	20.2	18.3
Specific surface area/$m^2\ g^{-1}$	86.0	79.7
TiO_2 weight[a]/mg cm^{-2} μm^{-1}	0.135 ± 0.003	0.173 ± 0.003
Roughness factor[b]/μm^{-1}	116 ± 3	138 ± 2
Absorbance at 540 nm[c]/μm^{-1}	0.159 ± 0.05	0.184 ± 0.06

[a] The weight-measurement sample area was 16 cm^2 with 15 μm thickness. [b] The roughness factor was obtained by multiplying specific surface area and TiO_2 weight. [c] Absorbance measurements were performed with a N719-adsorbed nanocrystalline TiO_2 layer at 540 nm. The optical background was obtained by using the same TiO_2 electrode after removal of N719 by soaking in 0.1 M *tert*-butylammonium hydroxide in acetonitrile. A cover glass plate was attached on the surface of the TiO_2 layer and the pores in the nanocrystalline TiO_2 layers were filled with butoxyacetonitrile to decrease the light scattering effect.

layer.[10] Although the specific surface area of nanoporous TiO_2 films decreased with $TiCl_4$ treatment, dye uptake becomes more efficient. These $TiCl_4$ effects about the decreasing specific surface area and the increasing absorbance at 540 nm coincide with previous reports.[5a,10] This disagreement between the variation of the dye absorption and the specific surface area can be simply explained by the increase of TiO_2 weight, because the roughness factor can be calculated by multiplying specific surface area and TiO_2 weight: in spite of the decrease of specific surface area with $TiCl_4$ treatment, the TiO_2 weight increased enough to increase the roughness factor. The ratios of (nano-TiO_2)/($TiCl_4$-treated nano-TiO_2) in roughness factor and absorbance at 540 nm were 1.19 and 1.16, respectively. This coincidence in relationship between roughness factor and absorbance suggests the enhancement of TiO_2 surface area by $TiCl_4$ treatment.

Fig.1 shows the dark current–voltage characteristics of the four kinds of mesoscopic-TiO_2 electrodes with and without adsorbed Ru dye. The onset of the dark current of <nano-TiO_2> occurred at low forward bias. Using a compact TiO_2 underlayer and a $TiCl_4$ treatment suppresses the dark current, shifting its onset by several hundred millivolts. This indicates that the triiodide reduction at the exposed part of FTO is responsible for the high dark current observed with the nanocrystalline TiO_2 film alone.

$TiCl_4$ treatments on underlayered films shifted the *I–V* curves to slightly lower voltages: from <UL/nano-TiO_2> to <UL/nano-TiO_2/$TiCl_4$> and from <UL/nano-TiO_2/Ru-dye> to <UL/nano-TiO_2/$TiCl_4$/Ru-dye> (Fig. 1b). This is attributed to increasing the electron trap site on the TiO_2 surface[11] with enlarging the surface area by $TiCl_4$ treatment (table 1). A similar effect was observed by Arakawa *et al.*; the dark current augmented by increasing the thickness of the nanocrystaline-TiO_2 electrode.[12]

Strikingly, adsorption of the N-719 <nano-TiO_2> electrode also suppresses the dark current (Fig. 1a) indicating that the Ru sensitizer itself worked as an effective "blocking layer" on FTO. On the other hand, the dark-current curves of <$TiCl_4$/nano-TiO_2/$TiCl_4$>, <UL/nano-TiO_2> and <UL/nano-TiO_2/$TiCl_4$> were shifted to slightly lower voltages by adsorption of N-719 (Fig. 1b) indicating that the sensitizer increases the dark current on electrodes where the FTO surface is already blocked. This is

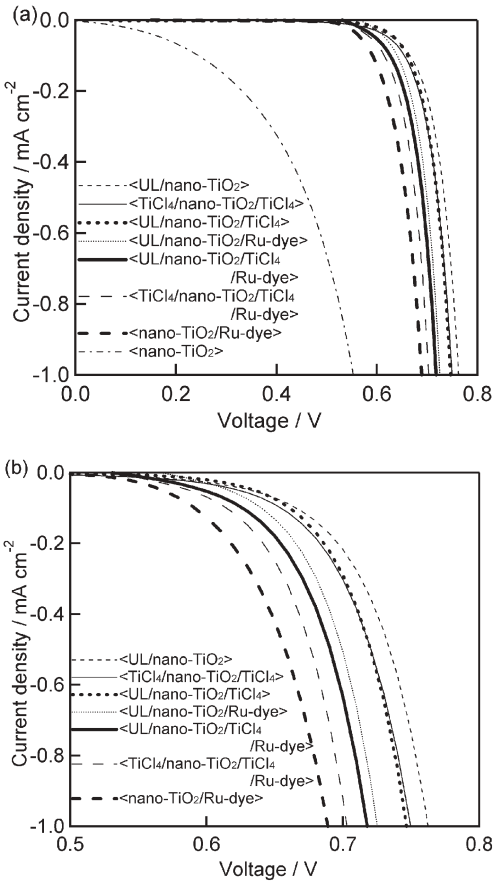

Fig. 1 (a) Dark current–voltage characteristics of mesoscopic TiO_2 electrodes in sandwich type cells with and without adsorbed Ru dye. The counter electrode was Pt-coated FTO. In Fig. 1b the abscissa is expanded in the 0.5–0.8 V range.

attributed to TiO_2 band shifting to positive values by surface protonation. The proton can be supplied by the Ru dye. We found the V_{OC} shifted by modifying the amount of proton on the Ru dye.[12b]

Photovoltaic results shown in Fig. 2 and the data summarized in Table 2 confirm the trends observed in the dark currents. The dye

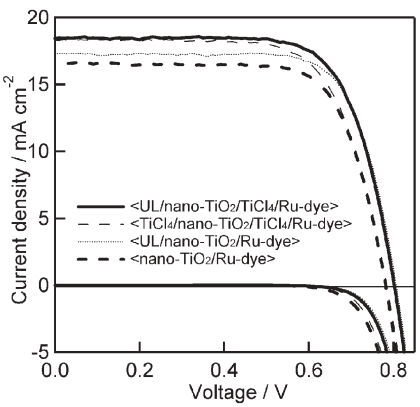

Fig. 2 Photovoltage–current characteristics curves of dye-sensitized solar cells by using four types of electrodes under a solar simulator (AM 1.5, 100 mW cm^{-2}).

Table 2 Photovoltaic characteristics of dye-sensitized solar cells with four types of TiO_2 electrodes. Each data was the average of three cells

Electrodes	J_{SC}/mA cm^{-2}	V_{OC}/V	*FF*	η(%)
<nano-TiO_2/Ru-dye>	16.6 ± 0.1	0.778 ± 0.06	0.731 ± 0.03	9.4 ± 0.2
<$TiCl_4$/nano-TiO_2/$TiCl_4$/Ru-dye>	18.2 ± 0.2	0.789 ± 0.03	0.704 ± 0.04	10.1 ± 0.1
<UL/nano-TiO_2/Ru-dye>	17.6 ± 0.2	0.805 ± 0.02	0.738 ± 0.05	10.5 ± 0.1
<UL/nano-TiO_2/$TiCl_4$/Ru-dye>	18.7 ± 0.1	0.798 ± 0.04	0.713 ± 0.05	10.6 ± 0.2

loaded nanocrystalline TiO_2 film alone gave the lowest conversion efficiency (Fig. 2, <nano-TiO_2/Ru-dye>). Introducing the compact TiO_2 underlayer in <nano-TiO_2/Ru-dye> increased the V_{OC} by 27 mV and the J_{SC} by 1 mA cm^{-2}. The difference between <nano-TiO_2/Ru-dye> and <UL/nano-TiO_2/Ru-dye> arose from suppressing the charge recombination by UL on FTO. A charge-recombination mathematical modelling carried out by Ferber *et al*[13] fits significantly with these *I–V* curves. Therefore, the observed improvement of V_{OC} and J_{SC} by using UL on FTO is in agreement with the theoretical calculations. An additional $TiCl_4$ treatment on <UL/nano-TiO_2> also increased the photocurrent by 0.9 mA cm^{-2}, resulting in decreases of fill factors due to the resistance of FTO, but the V_{OC} decreased slightly. The latter electrode <UL/nano-TiO_2/$TiCl_4$/Ru-dye> shows the best performance of 10.8% in conversion efficiency due to suppression of charge recombination by UL and enhancement of the surface area by $TiCl_4$ treatment. In spite of the small increase of V_{OC} when using UL (only by 10 mV) from <$TiCl_4$/nano-TiO_2/$TiCl_4$/Ru-dye> to <UL/nano-TiO_2/$TiCl_4$/Ru-dye>, the blocking effect of UL is necessary to obtain the high-efficiency DSC over 10.6%.

Although UL increased V_{OC} from that of non-underlayered nano-TiO_2 electrodes (table 2), the dark current–voltage characteristics of both electrodes of <$TiCl_4$/nano-TiO_2/$TiCl_4$> and <UL/nano-TiO_2/$TiCl_4$> show hardly any difference (Fig. 1(b)). Hence, the reduction by I_3^- at >700 mV under illumination/dark conditions should be considered separatedly; under illumination, the charge recombination occurred near the FTO substrate, on the other hand, under darkness, the I_3^- reduction by electron from TiO_2 electrode occurred at the surface of whole nanocrystalline TiO_2 electrodes. This phenomena under light and dark has been observed by IMIS[6] and electrical impedance spectroscopy,[14] respectively. Therefore, it is concluded that, in order to prevent the charge recombination near FTO surface at open-circuit photovoltage, the spray-coated compact TiO_2 underlayer is much more effective than the $TiCl_4$ pretreatment.

In conclusion, the Ru-sensitizer blocks the dark current at the FTO/electrolyte interface. The suppression of dark current is enhanced by introducing a compact layer between the FTO and the TiO_2 nanocrystals leading to an increase in the V_{OC}. $TiCl_4$ treatment improves the J_{SC} by enlarging the surface area of the mesoscopic film.

We are grateful to the Swiss Energy Office for support of this work.

Notes and references

1 A. J. Frank, N. Kopidakis and J. van de Lagemaat, *Coord. Chem. Rev.*, 2004, **248**, 1165.
2 K. Tennakone, G. R. R. A. Kumara, I. R. M. Kottegoda and V. P. S. Perera, *Chem. Comm.*, 1999, 15; A. Zaban, S. G. Chen, S. Chappel and B. A. Gregg, *Chem. Comm.*, 2000, 2231; A. Kay and M. Grätzel, *Chem. B*, 2002, **14**, 2930; E. Palomares, J. N. Clifford, S. A. Haque, T. Lutz and J. R. Durrant, *J. Am. Chem. Soc.*, 2003, **125**, 475; S. Ito, Y. Makari, T. Kitamura, Y. Wada and S. Yanagida, *J. Mater. Chem.*, 2004, **14**, 385.
3 B. A. Gregg, F. Pichot, S. Ferrere and C. L. Fieldes, *J. Phys. Chem. B*, 2001, **105**, 1422.
4 P. Wang, S. M. Zakeeruddin, P. Comte, R. Charvet, R. Humphry-Baker and M. Grätzel, *J. Phys. Chem. B*, 2003, **107**, 14336.
5 (*a*) A. Kay, thesis (No. 1214) in École Polytechnique Fédérale de Lausanne, Switzerland, (1994); (*b*) S. Ito, K. Ishikawa, C.-J. Wen, S. Yoshida and T. Watanabe, *Bull. Chem. Soc. Jpn.*, 2000, **73**, 2609; (*c*) P. J. Cameron and L. M. Peter, *J. Phys. Chem. B*, 2003, **107**, 14394; (*d*) P. J. Cameron and L. M. Peter, *J. Phys. Chem. B*, 2005, **109**, 930; (*e*) P. J. Cameron and L. M. Peter, *J. Phys. Chem. B*, 2005, **109**, 7392.
6 K. Zhu, E. A. Schiff, N.-G. Park, J. van de Lagemaat and A. J. Frank, *Appl. Phys. Lett.*, 2002, **80**, 685.
7 L. Kavan and M. Grätzel, *Electrochim. Acta*, 1995, **40**, 643.
8 U. Bach, D. Lupo, P. Comte, J. E. Moser, F. Weissörtel, J. Salbeck, H. Spreitzer and M. Grätzel, *Nature (London)*, 1998, **395**, 583.
9 (*a*) M. K. Nazeeruddin, S. M. Zakeeruddin, R. Humphry-Baker, M. Jirousek, P. Liska, N. Vlachopoulos, V. Shklover, Christian-H. Fischer and M. Grätzel, *Inorg. Chem.*, 1999, **38**, 6298; (*b*) M. K. Nazeeruddin, R. Humphry-Baker, P. Liska and M. Grätzel, *J. Phys. Chem. B.*, 2003, **107**, 8981.
10 S. Kambe, S. Nakade, Y. Wada, T. Kitamura and S. Yanagida, *J. Mater. Chem.*, 2002, **12**, 723.
11 R. Kato, A. Furube, A. V. Barzykin, H. Arakawa and M. Tachiya, *Coord. Chem. Rev.*, 2004, **248**, 1195; J. R. Durrant, S. A. Haque and E. Palomares, *Coord. Chem. Rev.*, 2004, **248**, 1247; J. Nelson and R. E. Chandler, *Coord. Chem. Rev.*, 2004, **248**, 1181.
12 Z.-S. Wang, H. Kawauchi, T. Kashima and H. Arakawa, *Coord. Chem. Rev.*, 2004, **248**, 1381.
13 J. Ferber, R. Stangle and J. Luther, *Sol. Energy Mater. Sol. Cells*, 1998, **53**, 29.
14 F. Fabregat-Santiago, J. Bisquert, G. Garcia-Belmonte, G. Boshloo and A. Hagfeldt, *Sol. Energy Mater. Sol. Cells*, 2005, **87**, 117.